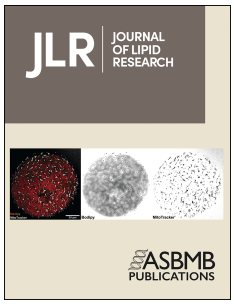

Helminth-induced prostaglandin signalling and dietary shifts in PUFA metabolism promote colitis-associated cancer.

Katherine A. Smith, Ella K. Reed, Irina Guschina, Victoria J. Tyrrell, Claire Butters, Matthew G. Darby, Brunette Katsandegwaza, Alisha Chetty, William GC. Horsnell, Valerie B. O'Donnell, Awen Gallimore

PII: S0022-2275(25)00097-5

DOI: https://doi.org/10.1016/j.jlr.2025.100837

Reference: JLR 100837

To appear in: *Journal of Lipid Research*

Received Date: 15 November 2024

Revised Date: 3 June 2025

Accepted Date: 4 June 2025

Please cite this article as: Smith KA, Reed EK, Guschina I, Tyrrell VJ, Butters C, Darby MG, Katsandegwaza B, Chetty A, Horsnell WG, O'Donnell VB, Gallimore A, Helminth-induced prostaglandin signalling and dietary shifts in PUFA metabolism promote colitis-associated cancer., *Journal of Lipid Research* (2025), doi: https://doi.org/10.1016/j.jlr.2025.100837.

Helminth-induced prostaglandin signalling and dietary shifts in PUFA metabolism promote colitis-associated cancer.

Katherine A Smith[1*], Ella K Reed[1], Irina Guschina[1], Victoria J Tyrrell[1], Claire Butters[2], Matthew G Darby[2], Brunette Katsandegwaza[3], Alisha Chetty[2], William GC Horsnell[4], Valerie B O'Donnell[1], Awen Gallimore[1]

[1]Cardiff University, Cardiff, UK

[2]University of Cape Town, Cape Town, South Africa

[3]University of Liege, Liege, Belgium

[4]Universtiy of Exeter, Exeter, UK

[*]Corresponding author: smithk28@cardiff.ac.uk

Short title

Helminth prostaglandin signalling exacerbates colon cancer.

Funding sources

This study was supported by the European Commission (grant number 657639) and the National Research Foundation of South Africa (grant number 99074). Awen Gallimore receives funding from Cancer Research UK (DRCRPG-NOV21-100003).

Abstract

Oxylipins derived from dietary polyunsaturated fatty acids (PUFAs) are key determinants of intestinal health, homeostasis and inflammatory disorders, such as colitis-associated colorectal cancer (CAC). Previous research has independently linked a high dietary omega (ω)-6:ω-3 PUFA ratio, or intestinal helminth infection, to an increased risk of CAC. However, whether these two factors interact to exacerbate disease risk and whether oxylipins contribute to this is unknown. In this study, we report that infection with the helminth *Heligmosomoides polygyrus bakeri* (Hpb) exacerbates tumour formation when combined with a high ω-6:ω-3 PUFA ratio diet. Dietary increases in tumour burden correlated with heightened levels of arachidonic acid (AA) and AA-derived lipoxygenase (LOX) oxylipins in the colon, including the 12/15-LOX product 12-hydroxyeicosatetraenoic acid, prior to disease onset. Although helminth infection further increased the production of 12/15-LOX oxylipins and increased expression of *Alox15*, responsible for producing these metabolites, inhibition of cyclooxygenase-dependent prostaglandin production with aspirin prevented helminth-exacerbation of disease. Helminth-infected mice exhibited increased phosphorylation of β-catenin in the colon, which was inhibited by EP2 and 4 antagonists. Moreover, administration of an EP agonist increased tumour burden in naive mice fed a high ω-6:ω-3 PUFA ratio diet, to the levels seen in helminth-exacerbation of disease. These data suggest that dietary changes in fatty acid composition coordinate with helminth-induced activation of EP signalling to exacerbate tumour development.

Keywords: Lipolysis and fatty acid metabolism, Omega-3 fatty acids, Phospholipids/Metabolism, Arachidonic acid, Lipoxygenase, Prostaglandins, Cell signalling, Colon.

Introduction

Colorectal cancer is the third most common cancer and the second leading cause of cancer-related death worldwide. In 2020, countries with the lowest human development index (HDI), which measures social and economic development, exhibited the lowest incidence of this disease compared to those with a very high HDI. However, projections for 2040 estimate a significant 103% increase in cases in low HDI countries, compared to a more moderate 35% increase anticipated in very high HDI countries (1). Many factors are thought to influence colorectal cancer development, including genetic risk as well as lifestyle choices. Patients with chronic inflammatory bowel disease (IBD) colitis are at an increased risk of developing colitis-associated colorectal cancer (CAC) (2-4), reflecting shared molecular mechanisms underlying these diseases.

Changes in diet are suggested to significantly impact colorectal cancer incidence (5, 6). Notably, its rise in low HDI countries has been linked with urbanisation, and the adoption of "Western" diets (7, 8), characterised by high ratios of ω-6:ω-3 polyunsaturated fatty acid (PUFA) that are now estimated to range between 20:1-50:1 (9). Diets rich in linoleic acid, an omega-6 (ω-6) PUFA, which is converted into arachidonic acid (AA) *in vivo*, are associated with increased IBD and colorectal cancer in humans and mouse models of disease (10-14). Murine studies have demonstrated a role for AA-derived oxylipins generated by cyclooxygenase (COX) in CAC using pharmacological tools such as aspirin, which also significantly reduces the risk of colorectal cancer incidence and improves disease-associated survival in humans (15, 16). However, high levels of oxylipins derived from AA by lipoxygenases (LOX) were reported in patient colon adenoma tissue samples (17) and several pre-clinical models have described the importance of 12/15-LOX-derived oxylipins, including 12-hydroxyeicosatetranoic acid (HETE), in promoting colorectal cancer cell growth and invasion (18-20). In line with the idea of shared mechanisms underlying disease in CAC and IBD, a significant reduction in dextran sulfate sodium (DSS) colitis in *Alox15*-deficient mice was linked to decreased production of 12-HETE, 15-HETE and 5-HETE (21).

Separate from diet, growing evidence indicates a positive association between helminth infection and colorectal cancer in humans and murine models (22-25). Soil-transmitted helminths (STH) are highly prevalent in low HDI countries, affecting an estimated 1.45 billion people worldwide (26). Recent studies in mice indicate that rodent STH transit through tissue can trigger COX and LOX-dependent oxylipin production from AA at that site following infection (27). In addition, a glutamate dehydrogenase enzyme found in the infectious larval products of the rodent STH *Heligmosomoides polygyrus bakeri* (Hpb) and larval cysts of the zoonotic tapeworm *Taenia*

Solium promoted PGE_2 production from macrophages and monocytes (28, 29). It is currently not known whether the oxylipins generated following helminth exposure contribute to colorectal cancer risk or progression of disease.

Mapping an increasing adoption of high ω-6:ω-3 ratio diets onto regions with high helminth infection rates, the question arises as to whether the combination of these factors further influences cancer incidence, and if so, whether oxylipins play a role. This is crucial to determine now, as helminth-endemic areas are reported to be undergoing a rapid nutritional transition to diets with a higher ω-6:ω-3 ratio (30, 31). To address whether both risk factors exacerbate disease by targeting the same oxylipin pathways, we tested the impact of a high ω-6:ω-3 ratio diet on tumour formation and oxylipin generation in mice in a model of DSS colitis-associated colorectal cancer (CAC), with or without concurrent helminth infection. The contribution of oxylipins generated by COX to driving CAC in this model is elucidated along with signalling mechanisms. Our data reveal two independent oxylipin pathways that are associated with an increased risk of colorectal cancer in mice: one that can be modified by diet and the other by the delivery of aspirin during helminth infection.

Materials and Methods

Experimental model details

Female 6-8-week-old mice were bred and maintained in-house under specific pathogen-free level 1-barrier conditions within a South African Veterinary Council (SAVC) authorized facility at the University of Cape Town (registration number FR15/14226). Serum and faecal screening revealed mouse norovirus, *Pasterella pneumotropica*, *Helicobacter spp*. and *Tritrichomonas muris*. Based on 369 of the 384 SNP loci, sequence genotyping of a tail snip from this strain by Charles River revealed a 90.2% match with the BALB/cByJ reference genome and an average 5.8% homozygous mismatch to this strain, including a 47.6% match to 129S4SvJae instead of a 45.2% match found for the reference BALBcByJ strain. Littermates were randomly assigned to experimental groups, housed within the same cage. Mice received standard laboratory chow containing low levels of ω-6 (Rodent Breeder, Cat. #RB2005, LabChef, Nutritionhub) and drinking water from weening *ad* libitum. Colitis-associated colorectal cancer was promoted in this strain using a pro-inflammatory high sucrose American Institute of Nutrition (AIN)-76A rodent diet (32). Animals were switched to an unmodified AIN-76A diet containing an ω-6:ω-3 ratio of 43:1 (Product #D10001, ResearchDiets, USA), a modified AIN-76A diet with a high ω-6:ω-3 ratio

of 120:1 (Product #D16083101, ResearchDiets, USA), or maintained on standard laboratory chow for one week before helminth infection or CAC induction. The composition of each diet is shown, where NG = not given by manufacturer (**Table 1**). Mice were then maintained in each diet until euthanasia. All protocols were approved by the University of Cape Town animal ethics committee (AEC 015/001, 019/010) and following SAVC authorisation (AR15/13922).

CAC induction

Azoxymethane (AOM) (Merck A5486) was delivered intraperitoneally (i.p.) at a dose of 8-12.5mg/kg followed by three fortnightly 5–7-day cycles of 2-2.5% 40,000-50,000 MW dextran sulfate sodium (DSS) (Affymetrix/USB J14489) in the water. 16, 16-dimethyl PGE_2 (dmePGE2) was administered i.p. to BALB/c mice at a dose of 12μg/kg and control mice received 200μl 1:1 DMSO:PBS. Low-dose aspirin was administered in the drinking water at a dose of 25mg/kg/day, given fresh every day. EP2 and EP4 antagonists PF-04418948 and ONO-AE3-208 were given i.p. at a dose of 10mg/kg at day -10, -7, -4 and -1 before AOM administration. 1:1 DMSO:PBS was given i.p. as a vehicle control. Mice were monitored daily for weight loss, physical, and behavioural changes and were immediately euthanised if the humane endpoint was reached. For tumour burden quantification, the entire colon was removed from below the cecum to the anus, measured and flushed with PBS and opened longitudinally before fixation in 4% paraformaldehyde. The colon was then pinned out before enumerating tumour burden macroscopically by an observer blinded to treatment group.

Helminth infection

Heligmosomoides polygyrus (bakeri) (Hpb) was maintained as described elsewhere (33). Mice were infected with 200 Hpb L3 larvae using a 21G gavage needle in 200μl of sterile water.

Oxylipin analysis

0.5cm tissue samples taken from the distal colon were snap frozen on dry ice, weighed and added to ceramic beads in 1ml anti-oxidant buffer containing 100μM diethylenetriaminepentaacetic acid (DTPA) and 100μM butylated hydroxytoluene (BHT) in phosphate buffered saline, as well as 2.1-2.9ng of 13(S)-HODE-d4, 5(S)-HETE-d8, 12(S)-HETE-d8, 15(S)-HETE-d8, 20-HETE-d6, LTB_4-d4, Resolvin D1-d5, PGE_2-d4, PGD_2-d4, $PGF_2\alpha$-d4, TXB_2-d4, 11-dehydro-thromboxane B2-d4 standard (Cayman chemicals). They were homogenised using a Bead Ruptor Elite for 2 x 20-second intervals at six m/s under cooled nitrogen gas (4°C). Lipids were extracted by adding a 2.5 ml solvent mixture (1 M acetic acid/isopropanol/hexane; 2:20:30, v/v/v) to 1 ml

homogenates in a glass extraction vial and vortexed for 60 sec. 2.5ml hexane was added to samples, and after vortexing for 60 seconds, tubes were centrifuged (500 xg for 5 min at 4℃) to recover lipids in the upper hexane layer (aqueous phase), which was transferred to a clean tube. Aqueous samples were re-extracted as above by the addition of 2.5 ml hexane, and the upper layers were combined. Lipid extraction from the lower aqueous layer was then completed according to the Bligh and Dyer technique (34). Specifically, 3.75ml of a 2:1 ratio of methanol: chloroform was added, followed by vortexing for 60 secs. Subsequent additions of 1.25ml chloroform and 1.25ml water were followed with a vortexing step for 60 seconds, and the lower layer was recovered following centrifugation as above and combined with the upper layers from the first stage of extraction. The solvent was dried under vacuum, and lipid extract was reconstituted in 200µl HPLC grade methanol. Lipids were separated by liquid chromatography (LC) using a gradient of 30-100% B over 20 minutes (A: Water: Mob B 95:5 + 0.1% Acetic Acid, B: Acetonitrile: Methanol – 80:15 + 0.1% Acetic Acid) on an Eclipse Plus C18 Column (Agilent) and analysed on a Sciex QTRAP® 6500 LC-MS/MS system. Source conditions: TEM 475°C, IS -4500, GS1 60, GS2 60, CUR 35 (**Supplemental Table S1)**. Chromatographic peaks were integrated using Multiquant 3.0.2 software (Sciex) (**Supplemental Figure S1**). The LOQ was signal: noise of at least 5:1 (LOD 3:1) and with at least 7 points across a peak. The ratio of analyte peak areas to internal standard was taken, and lipids were quantified using a standard curve made up and run at the same time as the samples. Each oxylipin was then standardised per mg of colon tissue. For data analysis, lipids with >50% of the values below the level of quantification (LOQ) were replaced with 1/5 of the minimum positive value of each variable and lipids where >50% of the values were below LOQ were removed from individual datasets (35).

Fatty acid analysis

Lipids were extracted using the Bligh and Dyer methods as above, then separated using one-dimensional thin-layer chromatography (TLC) on silica gel G plates (10 × 10 cm, Merck KGaA, Darmstadt, Germany) in the solvent system hexane/diethyl ether/acetic acid (80:20:1, *v*/*v*/*v*). Plates were sprayed with a 0.05% (*w*/*l*) 8-anilino-4-naphthosulphonic acid in dry methanol and viewed under U.V. light to reveal lipid classes. Lipid fractions were scraped from the plates and used for fatty acid methyl ester (FAME) preparation. FAMEs were prepared by transmethylation with 2.5% H_2SO_4 in dry methanol⁄toluene (2:1, *v*/*v*) at 70°C for 2 h. A known amount of nervonic acid (C24:1n9) was added as an internal standard, so that subsequent quantification of peaks (and, consequently, lipids) could be performed. FAMEs were extracted with HPLC-grade hexane after addition of 5% aqueous NaCl.

A Clarus 500 gas chromatograph with a flame ionizing detector (FID) (Perkin-Elmer 8500, Norwalk, CT, USA) and fitted with a 30 m · 0.25 mm i.d. capillary column (Elite 225, Perkin Elmer) was used for separation and analysis of FAs. The oven temperature was programmed as follows: 170°C for 3 min, programmed to 220°C at 4°C/min, hold for 15 min. FAMEs were identified routinely by comparing retention times of peaks with those of G411 standards (Nu-Chek Prep. Inc., Elysian, MN, USA). Perkin-Elmer Total Chrom Navigator software was used for data acquisition of the resulting chromatographs (**Supplementary Figure S2**).

Cell culture

The murine rectal carcinoma cell line CMT-93 (ATCC) was maintained in cultured in DMEM/F-12 (Thermo Fisher Scientific) supplemented with 10% fetal bovine serum, 1% non-essential amino acids, 1% L-glutamine, 100U/mL penicillin, 100U/mL streptomycin. Cells were confirmed as mycoplasma negative by using the LookOut® Mycoplasma PCR detection Kit (Sigma-Aldrich) and maintained for a maximum of 20 passages. Cells were seeded at in 6-well plates and grown to confluency before incubating in serum-free media for 24 hours before addition of 200 ng/mL 16, 16-dimethyl PGE_2 (dmePGE2) +/- EP2 and EP4 antagonists (PF-04418948 and ONO-AE3-208; 1μM). After 18 hours, cells were lysed in 1 x Pierce™ RIPA buffer containing 1x Halt™ Protease Inhibitor Cocktail (both Thermo Scientific) by passing through a 21-gauge needle 20-25 times on ice. The supernatant containing the protein fraction was removed by centrifugation at 9,600 x g for 15 minutes at 4°C. Protein concentration was determined using the Pierce™ BCA Protein Assay Kit (Thermo Scientific) before Western Blot analysis.

Western blotting

20μg of each protein sample was resolved using a 7.5% SDS-PAGE gel before being transferred to a polyvinylidene difluoride membrane (Bio-Rad). Membranes were washed with TBS 0.2% Tween, blocked in TBS supplemented with 0.2% Tween, 3% BSA and 0.5% gelatin for 30 mins and probed with specific antibodies overnight at 4°C. After three washes of 10 min in TBS 0.2% Tween, blots were incubated with Alexa Fluor 790-conjugated Donkey anti-rabbit IgG (H+L) (Jackson ImmunoResearch) (1/10,000) for 1 hr at room temperature, before imaging using the Li-Cor Odyssey cXL system (Li-Cor Biosciences). Densitometry readings were obtained using ImageJ to determine changes in protein expression. Primary antibodies used were: rabbit monoclonal β-

catenin (Cell Signalling, #8480) and rabbit polyclonal phospho-β-catenin (Ser552) (Cell Signalling, #9566), both 1/1000.

RNA sequencing

0.5cm tissue samples taken from the distal colon, weighed and added to RNAprotect tissue reagent (Qiagen) and stored overnight at -80. RNA was extracted using the RNeasy Mini Kit (Qiagen). RNA yield was quantified using the Qubit™ RNA BR assay kit between 185-289 ng/μL RNA with nanodrop spectrometry analysis revealing 260/280nm ratio of >2 and 260/230nm ratio of >1.9 for all samples. TapeStation Software (Agilent) revealed ribosomal integrity number (RIN) of 8.3-9.5 for all samples. Samples were made up to 20 ng/μL in nuclease-free water before library construction, quality control and Illumina next generation sequencing performed by Novogene (read length 150bp, read depth 30 million reads) (**Supplemental Table S2**). Paired-end clean reads were aligned to the *Mus musculus* BALB_cJ_v1 genome available from Ensemble (EMBL-EBI) (GCA_001632525.1) using Spliced Transcripts Alignment to a Reference (STAR) software, before using the Salmon tool to quantify transcript expression. MarkedDuplicates software analysis revealed high duplication levels and a technical issue in RNA sequencing in two samples (Naive 4 and Hpb 4), thus these samples were excluded from further downstream analysis. Comparison of gene expression between remaining samples was then performed using normalised counts, calculated by DESeq2 software.

qRT-PCR

Differences in gene expression found by RNA-seq were validated by qRT-PCR. 1 ug RNA was treated with RQ1 RNase-Free DNase (Promega), before transcribed using Moloney murine leukemia virus (MMLV) reverse transcriptase (Invitrogen). *Alox5* and *Alox15* mRNA levels were measured by real-time PCR using an Agilent technologies Mx3000P real-time PCR machine and primers designed using Integrated DNA Technologies (NCBI Reference Sequence: NM_009660.3 and NM_009662.2). The glyceraldehyde-3-phosphate dehydrogenase (GAPDH) gene was used as the reference gene with primers designed using NCBI primer blast (NCBI Reference Sequence: NM_001289726.2) (primer sequences given in **Supplemental Table S3**). Light Cycler PCR amplifications were carried out in 20 μl mixtures containing 4μL cDNA, 0.5μM primers, and 2×PowerUp™ SYBR™ green master mix (Applied Biosystems) using the following conditions: 15 s of denaturation at 95°C, 1

min of annealing of primers at 60°C, and 1 min of elongation at 72°C, for 45 cycles. The 2^-ΔΔCt method was used to calculate relative expression values between the gene of interest and the reference gene.

Quantification and statistical analysis

Data were assessed using the GraphPad Prism 10 software (La Jolla, CA). Data were tested for normal distribution using the Shapiro-Wilk test before statistical testing. For comparison between two groups with a normal distribution, an unpaired T-test was used, unless F test to compare variances revealed a difference in variance, at which point Welch's correction was applied. Where three or more groups were being tested, a parametric one-way analysis of variance (ANOVA) with Tukey's multiple comparison was applied. If data was not normally distributed, a non-parametric Mann-Whitney test or Kruskal-Wallis multiple comparison test was applied. ns on graphs denotes no statistical difference, where p-value *=$p<0.05$, **=$p<0.01$, ***=$p<0.001$ and ****= $p<0.0001$.

Volcano plot, heatmap analysis and pathway mapping.

Volcano plots of Log2 fold change and -Log10 p-value were generated using GraphPad Prism 10 software, following calculation of p-value (see statistical analysis) and fold change between each treatment condition. Heatmaps were also generated using GraphPad Prism 10 software following calculation of fold change between treatment conditions. Pathway mapping of oxylipins was based on that generated using the WikiPathways pathway collection metabolite database: metabolites_20210109 (36) with PathVisio software (37) in addition to published reviews (38, 39).

Results

A high ω-6:ω-3 ratio diet increased tumour burden in a murine model of colitis-associated colorectal cancer.

High dietary ratios of ω-6:ω-3 PUFAs have been linked with increased risk of colitis and colorectal cancer in both epidemiological studies and mouse models of disease (10-14). While some studies have found that increasing levels of ω-3 PUFA can reduce tumour development in a pre-clinical model of colitis-associated colorectal cancer (CAC) (14, 40), inconsistent results have been obtained when supplementing ω-3 or ω-6 in mouse models of colitis and spontaneous tumour formation (13, 41). Here, we address the impact of increasing the dietary ratio of ω-6:ω-3 on tumour development in a two-step model of CAC, by reducing levels of ω-3.

Mice were fed a chow diet lower in ω-6 PUFA (12g/kg), a high sucrose American Institute of Nutrition (AIN)-76A rodent diet higher in ω-6 PUFA (30g/kg, ω-6:ω-3 ratio of 43:1), or a modified AIN-76A diet with a higher ω-6:ω-3 ratio, due to lower levels of ω-3 PUFA (mAIN-76A, ω-6:ω-3 ratio of 120:1) for three weeks before induction of CAC, and continuing during the model (see **Table 1** for full details of diet). The purified AIN-76A diet serves as the base diet and more appropriate control for mAIN-76A compared to the grain-based chow diet, allowing for a more precise determination of how altering ω-6:ω-3 ratio influences tumour burden. CAC was induced by administering azoxymethane (AOM), combined with three 5-7-day cycles of dextran sulfate sodium (DSS) (**Figure 1A**) and body weight was monitored throughout the experiment. At ten weeks following administration of AOM, colon length was measured, and colon tumour burden was determined. Mice fed either AIN-76A or mAIN-76A diet, with 2.5 times the ω-6 PUFA content of chow, exhibited significantly increased tumour burden (**Figure 1B**) and shortening of the colon (**Figure 1C)** compared to mice fed a chow diet. Notably, tumour burden was significantly increased for mice consuming the mAIN-76A diet, with a higher ω-6:ω-3 ratio and containing less ω-3, compared to those consuming an AIN-76A diet (**Figure 1B**). In agreement with increased disease severity, mice fed the mAIN-76A diet exhibited significantly increased body weight loss compared to those receiving chow (**Figure 1D**).

A high ω-6:ω-3 ratio diet increased production of LOX oxylipins derived from the ω-6 PUFA arachidonic acid, while having no impact on COX-derived prostaglandins

Previous studies have found significant shifts in oxylipin production in the colon tissue of patients or animals with colorectal cancer, linking oxylipin production to development of disease (17, 42). Increases in dietary ω-3 were proposed to reduce spontaneous colorectal cancer development by elevating basal levels of eicosapentaenoic acid (EPA) and docosahexaenoic acid (DHA) within tissue phospholipid membranes and reducing the production of pro-inflammatory arachidonic (AA)-derived oxylipins, including prostaglandin E_2 (43). Since tumour development was lowest in mice fed a chow diet containing lower levels of ω-6 and highest in mice fed a mAIN-76A diet with a high ω-6:ω-3 ratio diet (**Figure 1B**), we then assessed whether risk of disease was associated with changes to oxylipins and their precursors in the colon tissue after 3 weeks of feeding, and prior to disease induction.

Lipidomics of the colon demonstrated that a high ω-6:ω-3 ratio diet resulted in a switch away from ω-3-derived oxylipins, to a profile dominated by oxylipins generated from the ω-6 PUFA arachidonic acid (AA) by LOX (**Figure 2A**). In mice fed a diet containing lower levels of ω-6, the most abundant oxylipins in the colon were 6-keto PGF1α, PGD_2 and PGE_2, followed by 13-hydroxyoctadecadienoic acid (HODE), 9-HODE, 11-HETE, $PGF_2\alpha$, 15-HETE and 12-HETE (**Figure 2B**). This is representative of a signature of oxylipins generated from arachidonic acid (AA) by COX (6-keto PGF1α, PGD_2, PGE_2, $PGF_2\alpha$) and 12/15-LOX (12-, 15-HETE), or from linoleic acid (LA) by 12/15-LOX (13-HODE), and is in line with the levels of oxylipins reported in control healthy mice fed a modified AIN-93G diet (42). High levels of 14- and 17-hydroxydocosahexaenoic acid (HDoHE) in mice fed a low ω-6 chow diet are consistent with their generation from the ω-3 PUFA DHA by 12/15-LOX (**Figure 2B**). 5-HETE and 5-hydroxyeicosapentaenoic (HEPE) from 5-LOX were also present at intermediate levels along with some oxylipins from cytochrome p450 (CYP), including 5(6)-epoxyeicosatrienoic acid (EET) and 12(13)-epoxyoctadecenoic acid (EpOME). Other lipids were present at lower relative amounts, particularly those with multiple oxygenations (**Figure 2B**).

Following consumption of a high ω-6:ω-3 ratio mAIN-76A diet, with lower levels of ω-3, there was a significant decrease in ω-3-derived oxylipins produced by LOX, COX and cytochrome p450 (CYP) (**Figure 2C-E**). All HEPEs derived from eicosapentaenoic acid (EPA) were significantly reduced, along with five out of eight detected HDoHEs from DHA (**Figure 2C, D left panel**). Two HDoHEs generated from 12/15-LOX (14-HDoHE and 17-HDoHE) (44) and non-enzymatic oxidation product (10-HDoHE), were unaffected by the diet (**Figure 2D right panel**). Levels of the ω-3, α-linolenic acid (ALA)-derived oxylipin produced by LOX, 9-hydroxyoctadecatrienoic acid (HOTrE), were also significantly decreased by this diet (**Figure 2E**). These significant decreases in ω-3-derived oxylipins were accompanied by a significant increase in several oxylipins produced by LOX from the ω-6 PUFA AA, including 5-, 12-, 15-HETE and 12-oxo-eicosatetraenoic acid (OxoETE) (**Figure 2F left panel**). There was also a significant increase in the levels of 8-HETE, most likely produced by the non-enzymatic oxidation of AA (**Figure 2F middle panel**).

Strikingly, there were no significant increases in the most abundant oxylipins produced by COX from the ω-6 PUFA AA in these mice, including 6-keto-PGF1α, PGD_2, PGE_2, $PGF_2\alpha$ and TXB_2 (**Figure 2F right panel**). An increase in AA-derived oxylipins was accompanied by a significant reduction in the linoleic (LA)-derived

oxylipin produced by CYP (12,13-DiHOME) (**Figure 2G**), suggesting that the generation of AA through dihomo-γ-linolenic acid (DGLA) is favoured following the consumption of a high ω-6:ω-3 ratio diet. Fatty acid analysis of these samples demonstrated significantly increased levels of the ω-6 PUFA precursor AA and significantly decreased levels of the ω-3 PUFA precursors EPA, docosapentaenoic acid (DPA) and DHA in the polar lipid fraction of colon samples from mice fed a high ω-6:ω-3 ratio mAIN-76A diet, when compared to mice fed a low ω-6 chow diet (**Figure 2H**). The analysis demonstrated the presence of all precursors in the polar lipid fraction, representing their incorporation into membrane phospholipids. In contrast, γ-linolenic acid (GLA) and EPA were below the level of detection in the triacylglycerol fraction, representing their absence or low levels in lipid stores (**Supplementary Figure S2A, B**). These data demonstrate that significant changes in oxylipin levels following dietary modification are linked to alterations in the composition of their precursors within tissue phospholipid membranes.

Combining helminth infection with a high ω-6:ω-3 ratio diet exacerbates tumour development.

Adoption of high ω-6:ω-3 ratio "Western diets" is increasing in areas endemic for soil-transmitted helminth (STH) infection (30, 31). A previous study found that infection with the rodent STH *Heligmosomoides polygyrus bakeri* (Hpb) increased CAC in the AOM/DSS model (24), therefore we aimed to determine how combining Hpb with differing diets might impact on tumour development. Mice fed either a low ω-6, or a high ω-6:ω-3 ratio diet were infected with Hpb after one week, then maintained on this diet throughout the experiment. CAC was induced two weeks after Hpb infection (**Figure 3A**). Whereas infection of mice fed a low ω-6 chow diet resulted in a non-significant trend toward increased tumour burden, infection of mice fed a high ω-6:ω-3 ratio diet significantly increased tumour burden and weight loss in mice (**Figure 3B, C**). Importantly, the tumour burden from combining a high ω-6:ω-3 ratio diet and Hpb infection (mean 17.1) was greater that adding the tumour burden of a high ω-6:ω-3 ratio diet (mean 8.8) to that of Hpb infection alone (mean 3.6) (**Figure 3B**), suggesting an interaction, or common mechanism may be enhancing tumour development between both factors in this model.

Combining helminth infection with a high ω-6:ω-3 ratio diet amplifies 12/15-LOX oxylipin production and increases expression of Alox15 and Alox5

Infection with a rodent helminth, or exposure to Hpb products, increased production of pro-inflammatory ω-6, AA-derived oxylipins *in vivo*, or *in vitro* models using murine and human macrophages (27, 28). Hpb

infection and exposure to Hpb products also increased the expression of oxylipin-generating enzymes *in vivo* and in *vitro* (28, 45, 46). After finding that AA-derived oxylipins produced by LOX correlate with dietary-dependent increases in tumour development (**Figure 2A, Figure 1B**), we were motivated to determine whether similar changes occurred during helminth exacerbation of disease. Corresponding to what was seen with a high ω-6:ω-3 ratio diet, Hpb infection of mice fed a high ω-6:ω-3 ratio diet resulted in significantly increased production of AA-derived oxylipins produced by 12/15-LOX, with 12-HETE becoming the most abundant oxylipin found in the colon (**Figure 4A, B**). The combination of Hpb infection and a high ω-6:ω-3 ratio diet had a synergistic effect on 8-HETE and 12-HETE levels, both derived from AA by either non-enzymatic oxidation or 12/15-LOX, respectively (**Fig 4C, D**). Unlike mice fed a high ω-6:ω-3 ratio diet alone, Hpb infection of mice fed a high ω-6:ω-3 ratio did not result in a shift away from ω-3-derived oxylipins and only production of 9,10-DiHOME, a CYP product of LA, was significantly reduced (**Figure 4E**). Instead, infection significantly increased production of several ω-3-derived oxylipins, including the 12/15-LOX products 12-HEPE, 15-HEPE and 14-HDoHE, and the non-enzymatic oxidation product 10-HDoHE (**Figure 4A-E**). Of note, 12/15-LOX oxylipin levels were also significantly increased in the colon of Hpb-infected mice fed a low ω-6 diet (**Figure 4D, Supplemental Figure S3D, E)**. As these mice were not prone to a significantly increased tumour development (**Figure 3B**), our data suggest that tumour burden was not solely linked to increased basal levels of the 12/15-LOX-derived oxylipins, following Hpb infection.

Because infection with the helminth *Taenia crassiceps* was previously shown to increase 12/15-LOX expression in peritoneal macrophages in response to interleukin(IL)-4 signalling (47), we hypothesised that Hpb may similarly promote 12/15-LOX oxylipin production through this pathway. RNA-seq and qRT-PCR validation of colon tissue demonstrated that expression of *Alox15* and *Alox5* was significantly increased in Hpb-infected mice fed a high ω-6:ω-3 ratio diet when compared to mice fed a high ω-6:ω-3 ratio diet alone (**Figure 4F, G**). However, expression of *Alox12*, *Alox12e*, *Alox8*, *Alox12b*, *Il13rα1*, *Il4rα*, *Il2rg and Il13* were not altered following Hpb infection (**Supplemental Figure S3A-C**).

Consistent with what was seen in mice fed a high ω-6:ω-3 ratio diet alone, the production of the most abundant AA-derived prostaglandins PGD_2, 6-keto-PGF1α, PGE_2 and PGF2α, was not significantly altered by Hpb infection of mice fed a low ω-6, or high ω-6:ω-3 ratio diet (**Supplemental Figure S3E-I**). Expression of

Ptgs1, Ptgs2 and *Ptges1* were similarly unaffected in the colon of Hpb-infected mice fed a high ω-6:ω-3 ratio diet (**Supplemental Figure S3J)**. As binding of PGE_2 to the PGE_2 receptor 2 (EP2), or EP4, can promote colorectal cancer (48, 49), the contribution of prostaglandin signalling to helminth-exacerbation of tumour formation was next assessed.

Aspirin administration significantly reduces Hpb-dependent exacerbation of CAC but has no impact on 12/15-LOX-derived oxylipin production.

Aspirin is thought to reduce the risk of colorectal cancer by inhibiting COX-dependent prostaglandin production and subsequent prostaglandin receptor signalling (48). To determine the contribution of prostaglandin signalling to helminth exacerbation of CAC, aspirin was administered at 25mg/kg/day in the drinking water starting one day before Hpb infection and continuing throughout the 14-day infection period. Mice were then restored to normal water and CAC was initiated by injecting AOM (**Figure 5A**). Uninfected (naive) mice fed a high ω-6:ω-3 ratio diet were also given aspirin for the equivalent period before injecting AOM, to determine any effect of treatment on CAC initiation. Aspirin treatment of Hpb-infected mice significantly reduced their heightened tumour burden, to the levels observed in uninfected mice fed a high ω-6:ω-3 ratio diet with CAC (**Figure 5B, Supplemental Figure S4A, B**). Weight loss and colon shortening were also significantly reduced following aspirin treatment of Hpb-infected mice, when compared to Hpb-infected mice receiving water (**Figure 5C, D**). Continuous administration of 25mg/kg/day aspirin during the AOM/DSS limited tumour development in mice, whereas administration from 4 days before AOM to 4 days after AOM had no significant impact on tumour formation (15). In line with these findings, aspirin delivery for two-weeks before AOM administration did not alter tumour formation, weight loss, or colon shortening in uninfected mice, suggesting that COX-dependent oxylipins were not involved in CAC development driven by a high ω-6:ω-3 ratio diet (**Figure 5B-D, Supplemental Figure S4A, B)**.

Lipidomics analysis of the colons from mice given aspirin for two weeks during helminth infection, or the equivalent period in uninfected controls, showed that aspirin significantly reduced levels of PGE_2 and TXB_2 in mice fed a high ω-6:ω-3 ratio diet, prior to disease onset (**Figure 5E, F**). PGE_2 levels were similarly reduced in Hpb-infected mice following aspirin treatment, although TXB_2 was less affected (**Figure 5E, F**). Pathway representation showed that aspirin suppressed levels of all other COX-derived oxylipins in both uninfected and

Hpb-infected mice (**Figure 5G**), including the more abundant ω-6-derived oxylipins 6-keto-PGF1α, PGD_2 and $PGF_2\alpha$ (**Figure 5H-J**), as well as the lower abundance oxylipins PGD1, PGE1 and 13,14-dihydro-15-keto PGE_2 (**Supplemental Figure S4C-E**). 11-HETE (a non-enzymatic product from AA) and 9-HODE (a non-enzymatic product from LA) were also significantly reduced by aspirin treatment as well as the low abundance ω-3-derived oxylipins, 11-HEPE, 13-, 16- and 20-HDoHE (**Supplemental Figure S4F-K**), which may be indicative of aspirin's ability to inhibit non-enzymatic oxidative stress (50). However, aspirin did not alter the increased production of 12/15-LOX products 12-HETE, 12-HEPE, 15-HEPE or 14-HDoDE found in Hpb-infected mice (**Figure 5K-N, Figure 4A**). Aspirin significantly reduced the production of the ω-6-derived oxylipins 15-HETE, 15-oxoETE and 15-HETrE in naive mice, but not in Hpb-infected mice (**Supplemental Figure S4L-N)**. 15-HETE is formed as the S-enantiomer by 12/15-LOX, or as a mixture of the 15(S)- and 15(R)-forms, by COX-1. Aspirin blocks COX-1-dependent production of 15(S)-HETE by platelets (51) and COX-2-dependent production of 15(R)-HETE (52). Therefore, our results suggest that 15-HETE is likely generated by COX in uninfected mice, whereas it is more likely to be generated by 12/15-LOX (53), following Hpb infection. In summary, aspirin inhibited COX-dependent oxylipin biosynthesis, while having no impact on 12/15-LOX products.

Enhanced prostaglandin receptor signalling exacerbated CAC and was increased following helminth infection of mice fed a high ω-6:ω-3 ratio diet.

The expression of nuclear p-β-catenin Ser^{552} has been linked to disease progression in the CAC AOM/DSS mouse model (54). COX-dependent oxylipin PGE_2 is reported to promote tumour development in $Apc^{Min/+}$ mice through EP2/4-dependent phosphorylation of β-catenin at Ser552 (p-β-catenin Ser^{552}) (55). As oral administration of the EP2 antagonist and oral delivery of the EP4 antagonist ONO-AE3-208 significantly reduced tumour burden and DSS-induced colitis, respectively, when given during disease development (48, 56), we hypothesised that Hpb exacerbation of CAC in mice fed a high ω-6:ω-3 ratio diet may be due to increased EP2/4-dependent signalling. The ratio of p-β-catenin Ser^{552} to β-catenin was quantified at day 64 following administration of AOM in Hpb-infected mice given a vehicle control (Veh) to Hpb-infected mice administered prostaglandin E_2 receptor 2 (EP2) and EP4 antagonists (PF-04418948, ONO-AE3-208; 10mg/kg) i.p. during Hpb infection (**Figure 6A**). Supporting the hypothesis, the ratio of p-β-catenin Ser^{552} to β-catenin was significantly increased in helminth-infected mice fed a high ω-6:ω-3 diet at day 64 following administration of AOM, when compared to naive controls (**Figure**

6B, C, Supplemental Figure S5A, B). Significantly, administration of EP2/4 antagonists to Hpb-infected mice prevented the helminth-driven phosphorylation of β-catenin at Ser552 (**Figure 6B, C, Supplemental Figure S5A, B**). To confirm our hypothesis, the PGE_2 analogue 16, 16-dimethyl PGE_2 (diMe-PGE_2) was administered to uninfected mice on a high ω-6:ω-3 diet, at days -10, -7, -4 and -1, followed by AOM administration (**Figure 6D)**. This is a competitive inhibitor of 15-hydroxy prostaglandin dehydrogenase (PGDH), which slows metabolism of PGE_2, and acts as an EP2, 3 and 4 agonist (57, 58). In the CAC model, diMe-PGE_2 significantly increased colon weight-to-length ratio and tumour burden of uninfected mice, reaching the level experienced by Hpb-infected mice (Veh) (**Figure 6E-G**). This indicates that PGE_2 signalling can increase tumour burden in a manner similar to the impact of Hpb infection in the CAC model (**Figure 6G**). Furthermore, these data provide further evidence that the impact of Hpb on tumour burden is mediated through increased prostaglandin E_2 receptor signalling, akin to diMe-PGE_2 administration. Since increased phosphorylation of β-catenin at Ser552 was observed following exposure of a human colorectal cancer cell line to PGE_2 (55), we determined whether dmPGE_2 mediated this effect through EP2/4-dependent signalling. Using a murine colorectal cancer cell line, the ratio of p-β-catenin Ser^{552} to β-catenin was increased following exposure to dmPGE_2. This effect was effectively inhibited by EP2/4 antagonists (**Figure 6H, I, Supplemental Figure S6A, B**). These results provide further support that dmPGE2 and Hpb infection promote tumourigenesis through EP2/4-signalling.

Discussion

Epidemiological evidence indicates that helminths or a high ω-6:ω-3 PUFA diet are independently associated with an increased risk of colorectal cancer in humans (10, 22, 25, 59, 60), however up until now, it was not known whether they could act in concert to further drive risk. Furthermore, how these two independent factors might mechanistically interact to influence the risk of CAC was not known. This is important since populations where helminth infections are most common are increasingly switching to high ω-6 diets (30, 31). Here, using a mouse model of CAC, we combine high ω-6:ω-3 diet with a rodent helminth infection and show a significantly increased tumour burden, which is mechanistically linked to helminth driven-PGE_2 signalling via EP2/4 receptors. While 12/15-LOX-derived oxylipin production from AA was elevated by both conditions, it was clear that basal levels of these oxylipins did not correlate with tumour burden. Because exacerbation of disease only occurs when

both factors were combined, our study proposes a direct interaction between two independent risk factors for CAC, one which is modifiable by diet and the other which is targetable through COX inhibition of oxylipin production.

First, we explored whether high ω-6:ω-3 PUFA ratios could impact the development of colorectal cancer using a pre-clinical colitis-associated colorectal cancer model, finding that reducing ω-3 content is linked to increased tumour burden. This is consistent with previous studies that have modified ω-6:ω-3 ratios through supplementation of the diet with ω-3, or the use of *fat-1* transgenic mice, which convert dietary ω-6 to ω-3 PUFAs (13, 14, 40, 43, 61, 62). These findings are significant because a shift towards a high ω-6:ω-3 ratio diet ranging between 20:1-50:1 in the West has been linked to the development of chronic inflammatory diseases, including colorectal cancer (9, 63-66). In low-HDI regions, the estimated lower ω-6:ω-3 ratio of 1:1-4:1 of traditional diets in rural areas has reflected lower colorectal cancer incidence (67). However, dietary patterns in these low-HDI regions are shifting towards to a Western ω-6:ω-3 ratio, coinciding with an estimated increase in colorectal cancer cases (1, 30, 31). Our data highlight the importance of maintaining a balanced ω-6:ω-3 PUFA ratio in both regions, to reduce the risk of cancer.

Our study further examined mechanisms driving tumour formation by measuring diet-driven levels of oxylipins in the colon, prior to tumour development. We found that a high ω-6:ω-3 ratio diet resulted in a switch away from ω-3-derived oxylipins, to a profile dominated by oxylipins generated from the ω-6 PUFA arachidonic acid (AA) by LOX, but not COX. As increases in dietary ω-3 PUFAs have previously been linked with a reduction in cancer development through lowering of AA levels within tissue phospholipid membranes and a decrease in the production of pro-inflammatory AA-derived prostaglandins (PG) (43), our results suggest that increased tumour burden in mice fed a high ω-6:ω-3 ratio diet may be driven by increased production of pro-inflammatory AA-derived oxylipins produced by LOX, due to reduced availability of ω-3-derived EPA and DHA substrate. Indeed, fatty acid analysis confirmed significantly increased AA and significantly reduced EPA and DHA in the colon of mice fed a high ω-6:ω-3 ratio diet. The lack of difference seen for AA-derived oxylipins produced by COX and their high abundance in the colon, may imply that COX is already saturated with AA, before switching to a high ω-6:ω-3 ratio diet. Diet-driven alterations to these pathways have been implicated in promoting tumour development, although given the nuances of different model types and sampling locations for oxylipins, it has not yet been possible to draw definitive conclusions linking changes in basal levels of oxylipins in the colon to disease

progression (40, 43, 61). While it remains to be determined how diet-induced alterations in basal levels of oxylipin production in the colon from a high ω-6:ω-3 diet are directly linked to tumour development, these findings underscore the need for dietary modifications to increase ω-3 intake and manage ω-6 levels, thereby reducing CRC development.

We then explored how helminth infection could further influence colorectal cancer in animals fed a low ω-6, or a high ω-6:ω-3 ratio diet. In a previous study, infection with *Heligmosomodies polygyrus bakeri* significantly increased tumour burden in the AOM/DSS mouse model of colitis-associated colorectal cancer (24). However, in our study, helminth infection of mice fed a low ω-6 diet did not result in a significant increase in tumour burden, nor did we observe high tumour burden in uninfected mice. This discrepancy may be due to the use of a mouse strain with reduced susceptibility to CAC or colitis (68-70), or to differences in the microbiota of mice maintained on a grain-based low ω-6 chow diet (71, 72). Notably, an increased tumour burden was observed in uninfected mice following the introduction of a modified AIN-76A diet, with a further increase upon helminth infection. These findings suggest that diet-dependent alterations in the microbiota may underlie the regulation of disease seen in our model. When helminth infection was combined with a high ω-6:ω-3 ratio diet, we observed further increases in the basal levels of 12/15-LOX oxylipins derived from AA. Whereas a shift in 12/15-LOX oxylipin production in mice fed a high ω-6:ω-3 ratio diet is likely due to the availability of substrate for the metabolic enzyme and saturation of enzymatic activity, these increases were likely mediated by increased *Alox15* expression following helminth infection. However, because 12/15-LOX oxylipins were significantly increased in the colon of helminth-infected mice fed a low ω-6 diet, which were not prone to increased tumour development, our data suggest that tumour burden was not solely linked to increased expression of *Alox15*, or the basal level of the 12/15-LOX-derived oxylipins following Hpb infection. Instead, helminth exacerbation of disease is more likely due to a coordinated response between pro-inflammatory signalling pathways activated by the AA-derived oxylipins favoured by a high ω-6:ω-3 ratio diet (e.g. 12-HETE and 8-HETE), and those promoted by helminth infection.

Like a high ω-6:ω-3 ratio diet, helminth infection of mice on a high ω-6:ω-3 ratio diet had no effect on COX-derived prostaglandin production in the colon, at least not at the time-points measured. Direct exposure to Hpb larval antigens triggered rapid production of PGE_2 within 24 hours (28), although all prostaglandins are

reported to have a short half-life, rapidly being oxidised and inactivated by 15-hydroxyprostaglandin dehydrogenase (15-PGDH) (73). By day 14 following infection with Hpb, the peak of prostaglandin production may have subsided and mice would be recovering from acute inflammation dominated by the production of LOX-derived oxylipins, as reported during the recovery phase of DSS treatment (74). Therefore, an extensive time-course would be needed to determine how Hpb infection in the small intestine influences prostaglandin production in the colon. Despite this, inhibition of COX-derived prostaglandin production with aspirin inhibited helminth-exacerbation of CAC, unlike the increased tumour burden seen in mice fed a high ω-6:ω-3 ratio diet alone. Because the impact of aspirin on prostaglandin levels was broadly similar regardless of Hpb infection, this finding supports the hypothesis that helminth exacerbation of tumour burden is not solely dependent on oxylipin production but may result due to coordination between downstream receptor signalling mediated by COX-derived products following Hpb infection, and pro-inflammatory signalling pathways activated by AA-derived oxylipins favoured by a high ω-6:ω-3 ratio diet. Aspirin treatment had no impact on increased 12/15-LOX oxylipins in helminth-infected mice, supporting the hypothesis that exacerbation of tumour burden was not dependent on Hpb-increases in *Alox15* expression and production of 12/15-LOX oxylipins alone. Although our study did not identify the cellular sources of specific oxylipins, previous research has highlighted the role of monocytes in producing COX-derived, but not LOX-derived oxylipins, following exposure to helminth antigens (28, 29). The expansion of 12/15-LOX expressing $CD11b^{+}Gr\text{-}1^{+}$ myeloid suppressor cells following helminth infection suggests that distinct cell types are responsible for LOX- and COX-derived oxylipin production in this context (47); however, further research is needed to confirm this.

Helminth infection was associated with increased activation of prostaglandin E_2 receptor EP2/EP4 signalling and administration of an EP receptor agonist increased tumour burden in naïve mice fed a high ω-6:ω-3 diet. These findings clearly implicate helminth activation of PGE_2 signalling in tumour formation via the EP2 and EP4 receptors. Signalling via EP2 and EP4 promoted tumour formation or colitis (48, 56), and we add to this by showing that helminth activation of EP2/4 is associated with increased tumour development. However, further research would be required to confirm whether helminth infection increases tumour burden through this pathway. A previous study has shown that exposure to the antigens of *Taenia solium (T. solium)* cysts can activate EP2 and EP4, thereby setting the precedent for helminth-driven increase in PGE_2 signalling (29). Activation of EP2/4

following exposure to this antigen is ascribed to a helminth glutamate dehydrogenase, also present in the larval antigens of Hpb (28, 29). Recent evidence shows that helminth glutamate dehydrogenase-dependent alterations in oxylipin production by macrophages are mediated through activation of p300 histone acetyltransferase and epigenetic regulation of immune regulatory genes (75). Although oxylipin signalling in rodents may differ in some respects from that in patients, many of our major findings are compatible with human studies. This includes the elevation 12/15- and 5-LOX derived oxylipins in tissue of colorectal cancer, and the lack of impact of aspirin supplementation (17) (Figure 2A, 4A and 5G), the increased phosphorylation of β-catenin on Ser-552 in patients with colorectal cancer (reviewed in (76)) and the activation of EP2/EP4 signalling following human helminth infection (reviewed in (77)) (Figure 6C). Whilst an epidemiological study would be required to determine whether a similar pathway occurs following Hpb infection in humans, these findings suggest that targeting prostaglandin signalling may help prevent the rising incidence of CAC in helminth-endemic areas adopting a "Western diet".

A key message of this study is that exacerbation of tumour burden is only seen when we combine Hpb infection with a high ω-6:ω-3 ratio diet. This suggests that two interlinked signals, one resulting from dietary-related increases in AA-derived LOX oxylipins and the other resulting from increased EP2/4 signalling due to Hpb infection, likely coordinate to result in exacerbation of disease. Further work is now needed to deconvolute the precise nature of this interaction. Given the challenges of deworming strategies and the delivery of aspirin to rural areas within low-HDI regions, it may be more effective to promote dietary modification as a strategy to prevent CAC in helminth endemic areas. Our data provides support that this strategy may mitigate the exacerbation of CAC due to the interaction between dietary changes and helminth infection in these regions.

Data availability: Data sources and handling of the publicly available datasets used in this study are described in the Materials and Methods. Example LC/MS/MS chromatograms, multiple reaction monitoring transitions, GC-FIT chromatographs, qRT-PCR primer details and raw western blots are contained within the supplemental information of the article. The RNA-seq data reported in this study are available at the Gene Expression Omnibus under the accession code GSE298815. Further information is available from the corresponding author upon request.

References

1. Ferlay J LM, Ervik M, Lam F, Colombet M, Mery L, Piñeros M, Znaor A, Soerjomataram I and Bray F. Global Cancer Observatory: Cancer Tomorrow (version 1.1). Lyon, France: International Agency for Research on Cancer. Available from: https://gco.iarc.who.int/tomorrow, accessed [30 August 2024]. 2024.
2. Clevers H. At the crossroads of inflammation and cancer. Cell. 2004;118(6):671-4.
3. Kim ER, Chang DK. Colorectal cancer in inflammatory bowel disease: the risk, pathogenesis, prevention and diagnosis. World J Gastroenterol. 2014;20(29):9872-81.
4. Lakatos PL, Lakatos L. Risk for colorectal cancer in ulcerative colitis: changes, causes and management strategies. World J Gastroenterol. 2008;14(25):3937-47.
5. McMichael AJ, McCall MG, Hartshorne JM, Woodings TL. Patterns of gastro-intestinal cancer in European migrants to Australia: the role of dietary change. Int J Cancer. 1980;25(4):431-7.
6. Le Marchand L, Wilkens LR, Kolonel LN, Hankin JH, Lyu LC. Associations of sedentary lifestyle, obesity, smoking, alcohol use, and diabetes with the risk of colorectal cancer. Cancer Res. 1997;57(21):4787-94.
7. Casari S, Di Paola M, Banci E, Diallo S, Scarallo L, Renzo S, et al. Changing Dietary Habits: The Impact of Urbanization and Rising Socio-Economic Status in Families from Burkina Faso in Sub-Saharan Africa. Nutrients. 2022;14(9).
8. Parkin DM, Nambooze S, Wabwire-Mangen F, Wabinga HR. Changing cancer incidence in Kampala, Uganda, 1991-2006. Int J Cancer. 2010;126(5):1187-95.
9. Mariamenatu AH, Abdu EM. Overconsumption of Omega-6 Polyunsaturated Fatty Acids (PUFAs) versus Deficiency of Omega-3 PUFAs in Modern-Day Diets: The Disturbing Factor for Their "Balanced Antagonistic Metabolic Functions" in the Human Body. J Lipids. 2021;2021:8848161.
10. Investigators IBDiES, Tjonneland A, Overvad K, Bergmann MM, Nagel G, Linseisen J, et al. Linoleic acid, a dietary n-6 polyunsaturated fatty acid, and the aetiology of ulcerative colitis: a nested case-control study within a European prospective cohort study. Gut. 2009;58(12):1606-11.

11. Lu Y, Li D, Wang L, Zhang H, Jiang F, Zhang R, et al. Comprehensive Investigation on Associations between Dietary Intake and Blood Levels of Fatty Acids and Colorectal Cancer Risk. Nutrients. 2023;15(3).

12. Hudert CA, Weylandt KH, Lu Y, Wang J, Hong S, Dignass A, et al. Transgenic mice rich in endogenous omega-3 fatty acids are protected from colitis. Proc Natl Acad Sci U S A. 2006;103(30):11276-81.

13. Whelan J, McEntee MF. Dietary (n-6) PUFA and intestinal tumorigenesis. J Nutr. 2004;134(12 Suppl):3421S-6S.

14. Nowak J, Weylandt KH, Habbel P, Wang J, Dignass A, Glickman JN, et al. Colitis-associated colon tumorigenesis is suppressed in transgenic mice rich in endogenous n-3 fatty acids. Carcinogenesis. 2007;28(9):1991-5.

15. Rohwer N, Kuhl AA, Ostermann AI, Hartung NM, Schebb NH, Zopf D, et al. Effects of chronic low-dose aspirin treatment on tumor prevention in three mouse models of intestinal tumorigenesis. Cancer Med. 2020;9(7):2535-50.

16. Figueiredo JC, Jacobs EJ, Newton CC, Guinter MA, Cance WG, Campbell PT. Associations of Aspirin and Non-Aspirin Non-Steroidal Anti-Inflammatory Drugs With Colorectal Cancer Mortality After Diagnosis. J Natl Cancer Inst. 2021;113(7):833-40.

17. Schmocker C, Gottschall H, Rund KM, Kutzner L, Nolte F, Ostermann AI, et al. Oxylipin patterns in human colon adenomas. Prostaglandins Leukot Essent Fatty Acids. 2021;167:102269.

18. Nguyen CH, Stadler S, Brenner S, Huttary N, Krieger S, Jager W, et al. Cancer cell-derived 12(S)-HETE signals via 12-HETE receptor, RHO, ROCK and MLC2 to induce lymph endothelial barrier breaching. Br J Cancer. 2016;115(3):364-70.

19. Chang J, Jiang L, Wang Y, Yao B, Yang S, Zhang B, et al. 12/15 Lipoxygenase regulation of colorectal tumorigenesis is determined by the relative tumor levels of its metabolite 12-HETE and 13-HODE in animal models. Oncotarget. 2015;6(5):2879-88.

20. Stadler S, Nguyen CH, Schachner H, Milovanovic D, Holzner S, Brenner S, et al. Colon cancer cell-derived 12(S)-HETE induces the retraction of cancer-associated fibroblast via MLC2, RHO/ROCK and Ca(2+) signalling. Cell Mol Life Sci. 2017;74(10):1907-21.

21. Kroschwald S, Chiu CY, Heydeck D, Rohwer N, Gehring T, Seifert U, et al. Female mice carrying a defective Alox15 gene are protected from experimental colitis via sustained maintenance of the intestinal epithelial barrier function. Biochim Biophys Acta Mol Cell Biol Lipids. 2018;1863(8):866-80.

22. Madbouly KM, Senagore AJ, Mukerjee A, Hussien AM, Shehata MA, Navine P, et al. Colorectal cancer in a population with endemic Schistosoma mansoni: is this an at-risk population? Int J Colorectal Dis. 2007;22(2):175-81.

23. Hayes KS, Cliffe LJ, Bancroft AJ, Forman SP, Thompson S, Booth C, et al. Chronic Trichuris muris infection causes neoplastic change in the intestine and exacerbates tumour formation in APC min/+ mice. PLoS Negl Trop Dis. 2017;11(6):e0005708.

24. Pastille E, Frede A, McSorley HJ, Grab J, Adamczyk A, Kollenda S, et al. Intestinal helminth infection drives carcinogenesis in colitis-associated colon cancer. PLoS Pathog. 2017;13(9):e1006649.

25. Katsidzira L, Gangaidzo IT, Makunike-Mutasa R, Manyanga T, Matsena-Zingoni Z, Thomson S, et al. A case-control study of risk factors for colorectal cancer in an African population. Eur J Cancer Prev. 2019;28(3):145-50.

26. Pullan RL, Smith JL, Jasrasaria R, Brooker SJ. Global numbers of infection and disease burden of soil transmitted helminth infections in 2010. Parasit Vectors. 2014;7:37.

27. Henkel FDR, Friedl A, Haid M, Thomas D, Bouchery T, Haimerl P, et al. House dust mite drives proinflammatory eicosanoid reprogramming and macrophage effector functions. Allergy. 2019;74(6):1090-101.

28. de Los Reyes Jimenez M, Lechner A, Alessandrini F, Bohnacker S, Schindela S, Trompette A, et al. An anti-inflammatory eicosanoid switch mediates the suppression of type-2 inflammation by helminth larval products. Sci Transl Med. 2020;12(540).

29. Prodjinotho UF, Gres V, Henkel F, Lacorcia M, Dandl R, Haslbeck M, et al. Helminthic dehydrogenase drives PGE(2) and IL-10 production in monocytes to potentiate Treg induction. EMBO Rep. 2022;23(5):e54096.

30. Imamura F, Micha R, Khatibzadeh S, Fahimi S, Shi P, Powles J, et al. Dietary quality among men and women in 187 countries in 1990 and 2010: a systematic assessment. Lancet Glob Health. 2015;3(3):e132-42.

31. Popkin BM. Global nutrition dynamics: the world is shifting rapidly toward a diet linked with noncommunicable diseases. Am J Clin Nutr. 2006;84(2):289-98.

32. Enos RT, Velazquez KT, McClellan JL, Cranford TL, Nagarkatti M, Nagarkatti PS, et al. High-fat diets rich in saturated fat protect against azoxymethane/dextran sulfate sodium-induced colon cancer. Am J Physiol Gastrointest Liver Physiol. 2016;310(11):G906-19.

33. Johnston CJ, Robertson E, Harcus Y, Grainger JR, Coakley G, Smyth DJ, et al. Cultivation of Heligmosomoides polygyrus: an immunomodulatory nematode parasite and its secreted products. J Vis Exp. 2015(98):e52412.

34. Bligh EG, Dyer WJ. A rapid method of total lipid extraction and purification. Can J Biochem Physiol. 1959;37(8):911-7.

35. Southam AD, Weber RJ, Engel J, Jones MR, Viant MR. A complete workflow for high-resolution spectral-stitching nanoelectrospray direct-infusion mass-spectrometry-based metabolomics and lipidomics. Nat Protoc. 2016;12(2):310-28.

36. Martens M, Ammar A, Riutta A, Waagmeester A, Slenter DN, Hanspers K, et al. WikiPathways: connecting communities. Nucleic Acids Res. 2021;49(D1):D613-D21.

37. Kutmon M, van Iersel MP, Bohler A, Kelder T, Nunes N, Pico AR, et al. PathVisio 3: an extendable pathway analysis toolbox. PLoS Comput Biol. 2015;11(2):e1004085.

38. Gabbs M, Leng S, Devassy JG, Monirujjaman M, Aukema HM. Advances in Our Understanding of Oxylipins Derived from Dietary PUFAs. Adv Nutr. 2015;6(5):513-40.

39. Litwack G. Chapter 8 - Eicosanoids. In: Litwack G, editor. Hormones (Fourth Edition): Academic Press; 2022. p. 195-212.

40. Jia Q, Lupton JR, Smith R, Weeks BR, Callaway E, Davidson LA, et al. Reduced colitis-associated colon cancer in Fat-1 (n-3 fatty acid desaturase) transgenic mice. Cancer Res. 2008;68(10):3985-91.

41. Matsunaga H, Hokari R, Kurihara C, Okada Y, Takebayashi K, Okudaira K, et al. Omega-3 fatty acids exacerbate DSS-induced colitis through decreased adiponectin in colonic subepithelial myofibroblasts. Inflamm Bowel Dis. 2008;14(10):1348-57.

42. Wang W, Yang J, Edin ML, Wang Y, Luo Y, Wan D, et al. Targeted Metabolomics Identifies the Cytochrome P450 Monooxygenase Eicosanoid Pathway as a Novel Therapeutic Target of Colon Tumorigenesis. Cancer Res. 2019;79(8):1822-30.

43. Petrik MB, McEntee MF, Johnson BT, Obukowicz MG, Whelan J. Highly unsaturated (n-3) fatty acids, but not alpha-linolenic, conjugated linoleic or gamma-linolenic acids, reduce tumorigenesis in Apc(Min/+) mice. J Nutr. 2000;130(10):2434-43.

44. Miyata J, Yokokura Y, Moro K, Arai H, Fukunaga K, Arita M. 12/15-Lipoxygenase Regulates IL-33-Induced Eosinophilic Airway Inflammation in Mice. Front Immunol. 2021;12:687192.

45. Nusse YM, Savage AK, Marangoni P, Rosendahl-Huber AKM, Landman TA, de Sauvage FJ, et al. Parasitic helminths induce fetal-like reversion in the intestinal stem cell niche. Nature. 2018;559(7712):109-13.

46. Drurey C, Lindholm HT, Coakley G, Poveda MC, Loser S, Doolan R, et al. Intestinal epithelial tuft cell induction is negated by a murine helminth and its secreted products. J Exp Med. 2022;219(1).

47. Brys L, Beschin A, Raes G, Ghassabeh GH, Noel W, Brandt J, et al. Reactive oxygen species and 12/15-lipoxygenase contribute to the antiproliferative capacity of alternatively activated myeloid cells elicited during helminth infection. J Immunol. 2005;174(10):6095-104.

48. Ma X, Aoki T, Tsuruyama T, Narumiya S. Definition of Prostaglandin E2-EP2 Signals in the Colon Tumor Microenvironment That Amplify Inflammation and Tumor Growth. Cancer Res. 2015;75(14):2822-32.

49. Hawcroft G, Ko CW, Hull MA. Prostaglandin E2-EP4 receptor signalling promotes tumorigenic behaviour of HT-29 human colorectal cancer cells. Oncogene. 2007;26(21):3006-19.

50. Hsu CS, Li Y. Aspirin potently inhibits oxidative DNA strand breaks: implications for cancer chemoprevention. Biochem Biophys Res Commun. 2002;293(2):705-9.

51. Rauzi F, Kirkby NS, Edin ML, Whiteford J, Zeldin DC, Mitchell JA, et al. Aspirin inhibits the production of proangiogenic 15(S)-HETE by platelet cyclooxygenase-1. FASEB J. 2016;30(12):4256-66.

52. Lecomte M, Laneuville O, Ji C, DeWitt DL, Smith WL. Acetylation of human prostaglandin endoperoxide synthase-2 (cyclooxygenase-2) by aspirin. J Biol Chem. 1994;269(18):13207-15.

53. Neilson AP, Ren J, Hong YH, Sen A, Smith WL, Brenner DE, et al. Effect of fish oil on levels of R- and S-enantiomers of 5-, 12-, and 15-hydroxyeicosatetraenoic acids in mouse colonic mucosa. Nutr Cancer. 2012;64(1):163-72.

54. Yang VW, Liu Y, Kim J, Shroyer KR, Bialkowska AB. Increased Genetic Instability and Accelerated Progression of Colitis-Associated Colorectal Cancer through Intestinal Epithelium-specific Deletion of Klf4. Mol Cancer Res. 2019;17(1):165-76.

55. Brudvik KW, Paulsen JE, Aandahl EM, Roald B, Tasken K. Protein kinase A antagonist inhibits beta-catenin nuclear translocation, c-Myc and COX-2 expression and tumor promotion in Apc(Min/+) mice. Mol Cancer. 2011;10:149.

56. Kabashima K, Saji T, Murata T, Nagamachi M, Matsuoka T, Segi E, et al. The prostaglandin receptor EP4 suppresses colitis, mucosal damage and CD4 cell activation in the gut. J Clin Invest. 2002;109(7):883-93.

57. Ohno H, Morikawa Y, Hirata F. Studies on 15-hydroxyprostaglandin dehydrogenase with various prostaglandin analogues. J Biochem. 1978;84(6):1485-94.

58. Kiriyama M, Ushikubi F, Kobayashi T, Hirata M, Sugimoto Y, Narumiya S. Ligand binding specificities of the eight types and subtypes of the mouse prostanoid receptors expressed in Chinese hamster ovary cells. Br J Pharmacol. 1997;122(2):217-24.

59. Bartsch H, Nair J, Owen RW. Dietary polyunsaturated fatty acids and cancers of the breast and colorectum: emerging evidence for their role as risk modifiers. Carcinogenesis. 1999;20(12):2209-18.

60. Azrad M, Turgeon C, Demark-Wahnefried W. Current evidence linking polyunsaturated Fatty acids with cancer risk and progression. Front Oncol. 2013;3:224.

61. Petrik MB, McEntee MF, Chiu CH, Whelan J. Antagonism of arachidonic acid is linked to the antitumorigenic effect of dietary eicosapentaenoic acid in Apc(Min/+) mice. J Nutr. 2000;130(5):1153-8.

62. Han YM, Jeong M, Park JM, Kim MY, Go EJ, Cha JY, et al. The omega-3 polyunsaturated fatty acids prevented colitis-associated carcinogenesis through blocking dissociation of beta-catenin complex, inhibiting COX-2 through repressing NF-kappaB, and inducing 15-prostaglandin dehydrogenase. Oncotarget. 2016;7(39):63583-95.

63. Simopoulos AP. The importance of the ratio of omega-6/omega-3 essential fatty acids. Biomed Pharmacother. 2002;56(8):365-79.

64. Blasbalg TL, Hibbeln JR, Ramsden CE, Majchrzak SF, Rawlings RR. Changes in consumption of omega-3 and omega-6 fatty acids in the United States during the 20th century. Am J Clin Nutr. 2011;93(5):950-62.

65. Calder PC. Polyunsaturated fatty acids and inflammation. Prostaglandins Leukot Essent Fatty Acids. 2006;75(3):197-202.

66. Poudyal H, Panchal SK, Diwan V, Brown L. Omega-3 fatty acids and metabolic syndrome: effects and emerging mechanisms of action. Prog Lipid Res. 2011;50(4):372-87.

67. Simopoulos AP. Essential fatty acids in health and chronic disease. Am J Clin Nutr. 1999;70(3 Suppl):560S-9S.

68. Suzuki R, Kohno H, Sugie S, Nakagama H, Tanaka T. Strain differences in the susceptibility to azoxymethane and dextran sodium sulfate-induced colon carcinogenesis in mice. Carcinogenesis. 2006;27(1):162-9.

69. Mahler M, Bristol IJ, Leiter EH, Workman AE, Birkenmeier EH, Elson CO, et al. Differential susceptibility of inbred mouse strains to dextran sulfate sodium-induced colitis. Am J Physiol. 1998;274(3):G544-51.

70. Nambiar PR, Girnun G, Lillo NA, Guda K, Whiteley HE, Rosenberg DW. Preliminary analysis of azoxymethane induced colon tumors in inbred mice commonly used as transgenic/knockout progenitors. Int J Oncol. 2003;22(1):145-50.

71. Laffin M, Fedorak R, Zalasky A, Park H, Gill A, Agrawal A, et al. A high-sugar diet rapidly enhances susceptibility to colitis via depletion of luminal short-chain fatty acids in mice. Sci Rep. 2019;9(1):12294.

72. Groschel C, Prinz-Wohlgenannt M, Mesteri I, Karuthedom George S, Trawnicek L, Heiden D, et al. Switching to a Healthy Diet Prevents the Detrimental Effects of Western Diet in a Colitis-Associated Colorectal Cancer Model. Nutrients. 2019;12(1).

73. Idborg H, Pawelzik SC. Prostanoid Metabolites as Biomarkers in Human Disease. Metabolites. 2022;12(8).

74. Hamabata T, Nakamura T, Masuko S, Maeda S, Murata T. Production of lipid mediators across different disease stages of dextran sodium sulfate-induced colitis in mice. J Lipid Res. 2018;59(4):586-95.

75. Bohnacker S, Henkel FDR, Hartung F, Geerlof A, Riemer S, Prodjinotho UF, et al. A helminth enzyme subverts macrophage-mediated immunity by epigenetic targeting of prostaglandin synthesis. Sci Immunol. 2024;9(102):eadl1467.

76. Amable G, Martinez-Leon E, Picco ME, Di Siervi N, Davio C, Rozengurt E, et al. Metformin inhibits beta-catenin phosphorylation on Ser-552 through an AMPK/PI3K/Akt pathway in colorectal cancer cells. Int J Biochem Cell Biol. 2019;112:88-94.

77. Oyesola OO, Tait Wojno ED. Prostaglandin regulation of type 2 inflammation: From basic biology to therapeutic interventions. Eur J Immunol. 2021;51(10):2399-416.

Tables

Table 1: Composition of rodent diets

Figure legends

Figure 1: A high ω-6:ω-3 ratio diet increased colitis-associated colorectal cancer (CAC).

Naive mice were fed a low ω-6 diet (chow), an AIN-76A control diet with higher ω-6 content (AIN-76A) or a modified AIN-76A diet with a higher ω-6:ω-3 ratio than AIN-76A (mAIN-76A) for three weeks before administration of 12.5mg/kg AOM at day 0 and three fortnightly cycles of 2.5% DSS in the water (**A**). This diet was then continued throughout the experiment. Tumour burden (**B**) and colon length was quantified at day 70 following AOM. Body weight was monitored throughout the experiment with % body weight of each individual standardized to 100% at day 5 following AOM (the start of the first DSS cycle) (**D**). Experiments shown are one representative from two experiments with n≥4 mice/group **(B-D)**. Unpaired T-test *p<0.05, **p<0.01, ***p<0.001, ****p<0.0001, error bars SEM.

Figure 2: A high ω-6:ω-3 ratio diet decreased oxylipin production derived from ω-3-PUFA and increased LOX oxylipin production derived from ω-6-PUFA.

Naive mice were fed a low ω-6 diet (chow), or a modified AIN-76A diet with a high ω-6:ω-3 ratio (mAIN-76A) for three weeks before lipidomic analysis of the colon. Simplified pathway representation of the Log_2 fold change of oxylipin for mice fed a high ω-6:ω-3 ratio diet, compared to those fed a low ω-6 diet as a heatmap scaled from highest amount (dark red, value 2.4) to lowest amount (dark blue, value -5.6) (**A**). Mean amount of each oxylipin in the colon of mice fed a low ω-6 diet was ranked (ng/mg tissue) (**B**). ng per mg amount of ω-3, eicosapentaenoic acid (EPA)-derived oxylipins 15-HEPE, 12-HEPE and 5-HEPE produced by LOX, 11-HEPE and 18-HEPE produced non-enzymatically, PGE_3 and PGD_3 produced by COX and 17,18-DiHETE and 14,15-DiHETE produced by cytochrome p450 (CYP) (**C**). ng per mg amount of ω-3, docosahexaenoic acid (DHA)-derived oxylipins 13-HDoHE, 20-HDoHE, 16-HDoHE, 4-HDoHE, 8-HDoHE, 14-HDoHE, 17-HDoHE and 10-HDoHE (**D**). ng per mg amount of ω-3, alpha-linolenic acid (ALA)-derived oxylipin 9-HOTrE (**E**) ng per mg amount of ω-6, arachidonic acid (AA)-derived oxylipins 12-HETE, 15-HETE, 5-HETE, 8-HETE and 12-oxoETE produced by LOX (left panel), or 6-keto PGF1α, PGD_2, PGE_2, PGF2α and TXB2 produced by COX (right panel) (**F**). ng per mg amount of ω-6, linoleic acid (LA)-derived oxylipin 12,13-DiHOME (**G**). μg per 100mg colon tissue of the ω-6 PUFA LA, GLA, DGLA, AA and the ω-3 fatty acids ALA, EPA, DPA and DHA, within the total polar lipid (membrane phospholipid) fraction (**H**). Experiments shown are pooled data from two experiments with n≥4 mice/group (**A-G**), or are one experiment with n≥4 mice/group (**H**). Unpaired T-test *p<0.05, **p<0.01, ***p<0.001, ****p<0.0001, error bars SEM.

Figure 3: Combining helminth infection with a high ω-6:ω-3 ratio diet exacerbated tumour development.

Naive mice were fed a low ω-6 diet (chow) or a modified AIN-76A diet with a high ω-6:ω-3 ratio than AIN-76A (mAIN-76A) for one week before infecting with 200 Hpb L3 larvae for 14 days (Hpb) or maintaining as naïve uninfected controls. AOM (12mg/kg) was then administered to all groups at day 0 followed by three fortnightly cycles of 2.5% DSS in the water (**A**) Both diets were maintained throughout the experiment. Colon tumour burden was determined at day 59 following administration of AOM (**B**). Body weight was monitored throughout the course of the experiment with % body weight of each individual standardized to 100% at day 5 following AOM (the start of the first DSS cycle) (**C**). Experiments shown are pooled data from two separate experiments with n≥4 mice/group. Unpaired T-test *p<0.05, **p<0.01, ***p<0.001, ****p<0.0001

Figure 4: Combining helminth infection with a high ω-6:ω-3 ratio diet amplified 12/15-LOX oxylipin production and increased expression of *Alox15* and *Alox5*.

Naive mice were fed a low ω-6 diet (chow) or a modified AIN-76A diet with a high ω-6:ω-3 ratio than AIN-76A (mAIN-76A) for one week, then infected with 200 Hpb L3 larvae for 14 days (Hpb), or maintained as naïve uninfected controls, before lipidomic or RNA-seq analysis of the colon. Simplified pathway representation of the Log_2 fold change of oxylipin for helminth infected mice fed a high ω-6:ω-3 ratio diet, compared to naïve mice fed a low ω-6 diet as a heatmap scaled from highest amount (dark red, value 2.4) to lowest amount (dark blue, value -2.3) (**A**) Mean amount of each oxylipin in the colon of helminth infected mice fed a high ω-6:ω-3 ratio diet was ranked (ng/mg tissue) (**B**). ng per mg amount of the oxylipins 8-HETE (**C**) and 12-HETE (**D**). Volcano plot of all colon oxylipins, highlighting those significantly increased (red symbols) or decreased (blue symbols) in helminth infected mice fed a high ω-6:ω-3 ratio diet, compared to naïve uninfected mice fed a high ω-6:ω-3 ratio diet (**E**). Dotted line represents $-Log_{10}$ p-value <0.05 (y-axis) and Log_2 Fold Change >2 (x-axis). Expression levels of *Alox15* and *Alox5* (**F**) and relative expression of *Alox15* and *Alox5* (**G**), in the colon of naïve and helminth infected mice fed a high ω-6:ω-3 ratio diet, taken at day 14 post-infection. Experiments shown are pooled data from two separate experiments with n≥4 mice/group (**A-E**), or one experiment with n=5 mice/group (**F-G**). Unpaired T-test *p<0.05, **p<0.01, ***p<0.001, ****p<0.0001, error bars SEM.

Figure 5: Administration of aspirin during helminth infection significantly reduced tumour burden and COX-dependent oxylipin production derived from AA.

All groups of mice were fed a high ω-6:ω-3 ratio diet throughout the experiment. One group was infected with 200 Hpb L3 larvae for 14 days (Hpb) (red symbols) and one group was maintained as uninfected (naive) controls (black symbols). 25mg/kg/day aspirin was delivered in the water from day -15 to day 0 of Hpb infection (purple symbols), or the equivalent time to uninfected (naive) mice (green symbols). Hpb-infected (red symbols) and uninfected (naive) mice (blue symbols) were maintained on normal drinking water. At day 0, aspirin-treated groups were placed onto water and CAC was initiated by

administering AOM at day 0, followed by three fortnightly cycles of DSS in the water (**A**). Tumour burden was quantified in the colon at day 59 following administration of AOM (**B**). Body weight was monitored throughout the experiment with % body weight of each individual standardised to 100% at day 5 following AOM (the start of the first DSS cycle) (**C**). Colon length was quantified in the colon at day 59 following administration of AOM (**D**). ng per mg amount of the oxylipins PGE_2 (**E**) and TXB2 (**F**) were quantified in the colon at day 0. Simplified pathway representation of the Log_2 fold change of oxylipins for uninfected (naive) mice treated with aspirin, compared to uninfected (naive) naïve maintained on water, or Hpb-infected mice treated with aspirin, compared to Hpb-infected mice maintained on water as a heatmap scaled from highest amount (dark red, value 1.4) to lowest amount (dark blue, value -5) (**G**). ng per mg amount of the oxylipins 6-keto PGF1α (**H**), PGD_2 (**I**), PGF2α (**J**), 12-HETE (**K**), 12-HEPE (**L**), 15-HEPE (**M**) and 14-HDoHE (**N**) in the colon at day 0. Experiments shown are pooled data from two experiments with n≥4 mice/group. Unpaired T-test *p<0.05, **p<0.01, ***p<0.001, ****p<0.0001, error bars SEM.

Figure 6: Enhanced prostaglandin receptor signalling increased CAC, to the same extent as helminth infection.

All groups of mice were fed a high ω-6:ω-3 ratio diet throughout the experiment. To determine whether helminth infection activated EP signalling, Hpb-infected mice were given 10mg/kg of the EP2 and EP4 antagonists PF-04418948 and ONO-AE3-208 i.p. at day -10, -7, -4 and -1 before AOM administration (Hpb EP2/4). Uninfected (Naive) and Hpb-infected (Hpb) were given 1:1 DMSO:PBS i.p. as a vehicle control. At day 0, CAC was initiated by administering AOM at day 0, followed by three fortnightly cycles of DSS in the water (**A**) Example western blot of pβ-catenin Ser552 and total β-catenin from the colon of mice for each treatment condition day 64 following administration of AOM (**B**). Graphical summary of the ratio of pβ-catenin Ser552 levels to total β-catenin levels for all treatment conditions (**C**). To determine the influence of EP activation on tumour burden, one group of mice was infected with 200

Hpb L3 larvae for 14 days (Hpb) (red symbols) and one group was maintained as uninfected (naive) controls (black symbols). Uninfected (naive) mice were given 12μg/kg of the EP agonist 16,16-dimethyl PGE_2 (dmPGE2) i.p. at day -10, -7, -4 and -1 before AOM administration (green symbols). Hpb-infected (red symbols) or uninfected (naive) mice (blue symbols) were given 1:1 DMSO:PBS i.p. as a vehicle control (Veh). At day 0, CAC was initiated by administering AOM at day 0, followed by three fortnightly cycles of DSS in the water (**D**). Body weight was monitored throughout the experiment with % body weight of each individual standardised to 100% at day 5 following AOM (the start of the first DSS cycle) (**E**). Colon weight to length ratio (mg/mm) (**F**) and tumour burden (**G**) were determined at day 61 following administration of AOM in Hpb-infected or uninfected (naive) mice receiving dmPGE2 or a vehicle control (Veh). The impact of EP2/EP4 antagonists (PF-04418948, ONO-AE3-208; 1μM) on $dmPGE_2$-induced increases in phosphorylation of β-catenin at Ser552 was assessed in a CMT-93 cell line. Example western blot of pβ-catenin Ser552 and total β-catenin from CMT-93 cells treated with dmPGE2 (200 ng/mL) +/- EP2/4 inhibitors (1μM) (**H**). Graphical summary of the ratio of pβ-catenin Ser552 levels to total β-catenin levels for all treatment conditions (**I**). Experiments shown are pooled data from two separate experiments with n≥4 mice/group (**E-G**), are one experiment with n=5 mice/group (**B-C**), or are pooled data from four separate experiments with n=1/group (**I**). Unpaired T-test *$p<0.05$, **$p<0.01$, ***$p<0.001$, ****$p<0.0001$, error bars SEM.

Diet	Standard Laboratory Chow		AIN-76A		Modified AIN-76A	
Product #	**2005**		**D10001**		**D16083101**	
Component	**g/kg**	**g%**	**g/kg**	**g%**	**g/kg**	**g%**
Protein	220	22 (soybean, maize protein concentrate, fishmeal)	200	20 (casein)	200	20 (casein)
Carbohydrate	520	52 (maize, wheat bran, soybean, sucrose)	660	66 (corn starch, sucrose, cellulose)	660	66 (corn starch, sucrose, cellulose)
Fiber	40	4 (soybean)	50	5 (all cellulose)	50	5 (all cellulose)
Fat	50	5 (maize, soybean, wheat bran)	50	5 (corn oil)	50	5 (sunflower oil, high linoleic)
Ingredient	**g/kg**	**g%**	**g/kg**	**g%**	**g/k50g**	**g%**
Linoleic acid (ω-6)	12	1.2	30.05	3.005	30.1	3.01
α-linolenic acid (ω-3)	NG	NG	0.7	0.07	0.25	0.025
Sucrose	40-60	4-6	500	50	500	50
ω-6:ω-3 ratio	NG		42.9:1		120.4:1